Research article

The therapeutic effect and targets of *herba Sarcandrae* on breast cancer and the construction of a prognostic signature consisting of inflammation-related genes

Jie Yuan [a,b,*,1], Minxia Lin [a,1], Shaohua Yang [a,b], Hao Yin [b], Shaoyong Ouyang [b], Hong Xie [b], Hongmei Tang [c], Xiaowei Ou [b], Zhiqiang Zeng [a,b,**]

[a] *Department of General Surgery, Foshan Clinical Medical School, Guangzhou University of Chinese Medicine, Foshan, China*
[b] *Department of General Surgery, Foshan Fosun Chancheng Hospital, Foshan, China*
[c] *Pharmaceutical Department, First Affiliated Hospital of Guangzhou University of Chinese Medicine, Guangzhou, China*

ARTICLE INFO

ABSTRACT

Background: The prevalence of breast cancer (BRCA), which is common among women, is on the rise. This study applied network pharmacology to explore the potential mechanism of action of *herba sarcandrae* in BRCA and construct a prognostic signature composed of inflammation-related genes.
Methods: The active ingredients of *herba sarcandrae* were screened using the SymMap, TCMID, and TCMSP platforms, and the molecular targets were determined in the UniProt database. The "drug-active compound-potential target" network was established with Cytoscape 3.7.2. The molecular targets were subjected to disease ontology, gene ontology (GO), and Kyoto Encyclopedia of Genes (KEGG) analyses. AutoDock software was used for molecular docking. Differentially expressed genes (DEGs) related to inflammation were obtained from the BRCA Cancer Genome Atlas (TCGA) database. In the training cohort, the univariate Cox regression model was applied to preliminarily screen prognostic genes. A multigene signature was built by the least absolute shrinkage and selection operator (LASSO) regression model, followed by validation through Kaplan–Meier, Cox, and receiver operating characteristic (ROC) analyses.
Results: Forty-one active compounds were identified, and 265 therapeutic targets for *herba sarcandrae* were predicted. GO enrichment results revealed significant enrichment of biological processes, such as response to xenobiotic stimuli, response to nutrient levels, and response to lipopolysaccharide. KEGG analysis revealed significant enrichment of pathways such as AGE-RAGE and chemical carcinogenesis receptor activation signaling pathways. In addition, *the herbs Marc-Andre* and rutin were shown to mediate BRCA cell proliferation and apoptosis via the interferon regulatory factor 1 (IRF1)/signal transducer and activator of transcription 3 (STAT3)/programmed death-ligand 1 (PD-L1) pathway. Sixteen inflammatory signatures, including BST2, GPR132, IL12B, IL18, IL1R1, IL2RB, IRF1, and others, were constructed, and the risk score was found to be a strong independent prognostic factor for overall survival in BRCA patients. The 16-

inflammation signature was associated with several clinical features (age, clinical stage, T, and N classifications) and could reflect immune cell infiltration in tumor microenvironments with different immune cells.

Conclusions: Herba sarcandrae and *rutin* were shown to mediate BRCA cell proliferation and apoptosis via the IRF1/STAT3/PD-L1 pathway, and the 16-member inflammatory signature might be a novel biomarker for predicting BRCA patient prognosis, providing more accurate guidance for clinical treatment prognosis evaluation and having important reference value for individualized treatment selection.

1. Introduction

Breast cancer (BRCA) is a leading cancer affecting females worldwide, carrying a significant socioeconomic burden [1,2]. Although the prognosis of many patients with BRCA may improve compared with that of patients with other solid tumors receiving multiple treatments, including radical surgery, chemotherapy, radiotherapy, and targeted therapy, some patients with BRCA achieve adverse outcomes [3]. The complexity of the molecular mechanisms that regulate tumorigenesis and progression determines the heterogeneity of BRCA, and the choice of treatment regimen and disease prognosis is subject to this heterogeneity [4]. Molecular advances have allowed a deeper comprehension of the cellular pathways that control BRCA development, facilitating advances in identifying diagnostic markers and developing new therapeutic strategies [5]. The identification of new drugs for BRCA and the establishment of tools with accurate prognostic predictors for patients with BRCA are essential for guiding clinical management.

TCM *herba sarcandrae* is a dried whole grass of grass corals belonging to the Chloranthaceae family and is commonly used to treat a variety of diseases [6]. Multiple compounds, such as coumarins, phenolic acid flavonoids, and sesquiterpenes, have been isolated and identified from *herba sarcandrae* [7]. Pharmacological studies have confirmed that *herba sarcandrae* extracts have anti-thrombocytopenia, anti-tumor, anti-inflammatory, and other effects [8]. Due to the complexity of the chemical composition of plant extracts and the synergistic effects of various chemical components, as well as the fact that various chemical components interact with many targets, it is difficult to understand the molecular mechanisms by which they act on certain molecular targets. In particular, its antitumor effect has been clinically confirmed [9]. For instance, *uvangoletin* extracted from *herba sarcandrae* can induce HepG2 cell apoptosis and autophagy, resulting in the inhibition of HepG2 cell proliferation and metastasis through the protein kinase B/mammalian target of rapamycin, mitogen-activated protein kinase (MAPK), and transforming growth factor-beta/SMAD family member 2 signaling pathways [10]. *Rosmarinic acid* extracted from *herba sarcandrae* repressed MDA-MB-231 cell proliferation, migration and facilitated apoptosis, which may be associated with B-cell lymphoma-2 (Bcl-2) and Bax (Bcl2-associated X) protein levels [11]. *Ethyl acetate* obtained from *herba sarcandrae* induced cell cycle arrest and increased the Bax/Bcl-2 ratio in leukemic HL-60 cells [12]. Although *herba sarcandrae* has been revealed to have anti-tumor effects on BRCA, the active ingredients and molecular mechanisms of *herba sarcandrae* against tumors are unclear and need to be further studied.

Biomarkers based on inflammatory responses or signaling pathways are expected to predict survival and guide the design of personalized therapies for BRCA patients [13]. This is primarily due to the effect of inflammation on the tumor phenotype and clinical treatment efficacy [14]. Inflammation has become one of the main markers of cancer progression [15] and plays key roles in tumor initiation and outcome [16,17]. However, in the field of clinical management, there are still knowledge gaps regarding the ability of inflammation-specific prognostic features to predict long-term survival in patients with BRCA.

Therefore, we used network pharmacology methods to identify gene targets and pathways involved in the interaction between *herba sarcandrae* and BRCA and to investigate the effect of herba sarcandrae and its active ingredient *rutin* on BRCA cell malignancy. By utilizing bioinformatics technology to mine and obtain RNA and clinical data from the BRCA-TCGA database, differentially expressed genes (DEGs) related to inflammation were screened, and prognostic models were constructed to compare significant differences in survival between the high-risk and low-risk groups.

2. Materials and methods

2.1. Screening of active ingredients and prediction of targets in herba sarcandrae

Multiple drug-related databases for symptom mapping (SymMap, http://www.symmap.org/), the Traditional Chinese Medicine integrative database (TCMID, http://www.megabionet.org/tcmid/), and Traditional Chinese Medicine Systems Pharmacology (TCMSP, https://old.tcmsp-e.com/tcmsp) were used to retrieve the relevant targets of the active ingredients of *herba sarcandrae*, and the targets were converted into corresponding genes with the help of the UniProt database (https://www.uniprot.org/).

2.2. Construction of the "drug-active compound-potential target (Dacpt)" network

The Dacpt network was established by Cytoscape 3.7.2 (https://cytoscape.org/). For this network, both active compounds and potential targets of *herba sarcandrae* were included. Node colors and sizes were fashioned based on degree values.

2.3. Disease ontology (DO), gene ontology (GO), and Kyoto Encyclopedia of Genes and Genomes (KEGG) enrichment analyses

DO, GO, and KEGG enrichment analyses of the relevant targets of the active ingredients of *herba sarcandrae* were carried out by the "cluster Profiler" package ($P < 0.05$). The diseases associated with the targets of *herba sarcandrae* active ingredients were identified through DO analysis. The biological processes, molecular functions, and cellular components related to the targets of *herba sarcandrae* active ingredients were identified through GO analysis. In addition, KEGG analysis identified the signaling pathways enriched by active ingredient potential targets of *herba sarcandrae*.

2.4. Screening of differentially expressed genes (DEGs) linked to the inflammatory response in BRCA

Clinical and transcriptome expression data associated with BRCA were downloaded from the Gene Expression Omnibus (GEO) and The Cancer Genome Atlas (TCGA) (https://portal.gdc.cancer.gov/) databases. Clinical data were collected and summarized using the "limma" package in R software to construct an expression matrix related to the inflammatory response. The screening of DEGs was performed according to a false discovery rate (FDR) < 0.05 and a $|\log_2$-fold change (FC) $| \geq 0.585$. Kaplan–Meier plots were generated for overall survival (OS) analysis.

2.5. Docking and verification of potential active ingredients with core target molecules

Mol*2 files were downloaded from the PubMed database. The PDB format of the core protein domains was downloaded from the PDB database (http://www.rcsb.org/). The LibDock module of Discovery Studio 2019 was used to complete the virtual screening as follows: water molecules were removed, and DS2019 was applied to minimize protein and ligand energy. For the correct ionization n and tautomeric states of amino acid residues, all nonpolar hydrogens are merged (removed), and partial atomic charges are assigned using the Gasteiger–Marsili method. Molecular docking was further performed to evaluate the possible binding mode between the *herba sarcandrae* component and the core protein binding site. The three compounds with the highest LibDockScore values were selected for subsequent binding energy and RMSD calculations as follows: PyMOL software was used to dehydrate and dephosphate the protein. AutoDockTools 1.5.7 software was used to convert the PDB format of the top 6 most active drug components and the core protein-encoding gene files into pdbqt format. A Vina script was used to calculate the molecular binding energy and display the molecular docking results. The molecular docking results of the ligand–receptor complex were displayed in 3D and 2D to evaluate the reliability of the bioinformatics analysis.

Data on the underlying active components of rutin were retrieved from the TCMSP database. The 3D structures of TRF1 docking targets were determined with the Worldwide Protein Data Bank (PDB) database (https://www.rcsb.org/). The PDB ID is 4CRL. The docking results were visualized using AutoDock Tools in conjunction with PyMol software.

2.6. Cell culture

The mouse BRCA cell line 4T1 (CL-0007, Procell, Wuhan, China) and the human BRCA cell line MDA-MB-231 (human) (CL-0150, Procell) were cultured in Roswell Park Memorial Institute (RPMI)-1640 medium (Procell) and Leibovitz's L-15 medium (Procell) supplemented with 10 % fetal bovine serum (FBS; Thermo Fisher Scientific, Pittsburgh, PA, USA) and 1 % penicillin–streptomycin (ScienCell, San Diego, California, USA), respectively, in a humid incubator at 37 °C and 5 % CO_2.

2.7. Cell counting Kit-8 (CCK-8)

4T1 (mouse) and MDA-MB-231 (human) cell lines were seeded and treated with concentrations of Epimedin C (#HY-N0260, MCE, USA), rutin (#N1833, APExBIO, USA), or β-sitosterol (#N1688, APExBIO) (0, 10, 50, 100, 500, 500 μM) for 48 h. Ten microliters of CCK-8 reagent (#G4103, Servicebio, Wuhan, China) were added. The absorbance at 450 nm was measured using a microplate reader (Thermo).

2.8. Flow cytometry assay

BRCA cell lines were seeded in 96-well plates and treated with rutin (0, 10, 50, 100, 500, or 500 μM) for 48 h. Assays for apoptosis were performed using an Annexin-V-FITC and propidium iodide (PI) double-staining kit (#100-101-100, GOONIE, Guangzhou, China) based on the manufacturer's instructions. Ultimately, the detection of stained cells was accomplished by flow cytometry (Miltenyi BiotecTM FACS Quant 10; Milteny Biotech, Germany). The extracted data were analyzed using FlowJo software (Tree Star, San Carlos, CA).

2.9. Coimmunoprecipitation (Co-IP)

BRCA cell lines treated with or without rutin (50 μM) were lysed in RIPA buffer. Lysates and corresponding antibodies were incubated overnight (4 °C). Then, magnetic beads (MCE, HY-K0208, treated with 3 % BSA before use) were incubated with protein-antibody complexes overnight at 4 °C. The beads were washed 5 times with precooled wash buffer, followed by the addition of 5 × sample buffer and cooking at 95 °C for 10 min. The supernatant was extracted by centrifugation (12,000 rpm, 15 min, 4 °C). The

relevant proteins were analyzed by western blotting.

2.10. Western blotting

Total protein was extracted using a protein extraction kit (#P0013C, RIPA Lysis Buffer, Beyotime). The protein concentration was measured using the BCA method (Biosharp BL521A). Equal amounts of proteins (30 μg) were separated and transferred to PVDF membranes. Following encapsulation in 5 % skim milk, the PVDF membranes were incubated with the following primary antibodies: anti-IRF1 (1:1000, #a7692, ABclonal, Wuhan, China), anti-phospho-(Ser/Thr) Phe (1:1000, Cell Signaling Technology, #9631), anti-STAT3 (1:1000, #10253-2-ap, Proteintech, Wuhan, China), anti-phospho-STAT3-Y705 (1:200, #AP0070, ABclonal), anti-PD-L1 (1:1000, #A1645, ABclonal), and GAPDH (1:50000, #60004-1-Ig, Proteintech). Following incubation with secondary antibodies (#BL003A/#BL001A, Biosharp, Beijing, China), an enhanced chemiluminescence (ECL) system was used to visualize the protein bands, followed by quantification with ImageJ software.
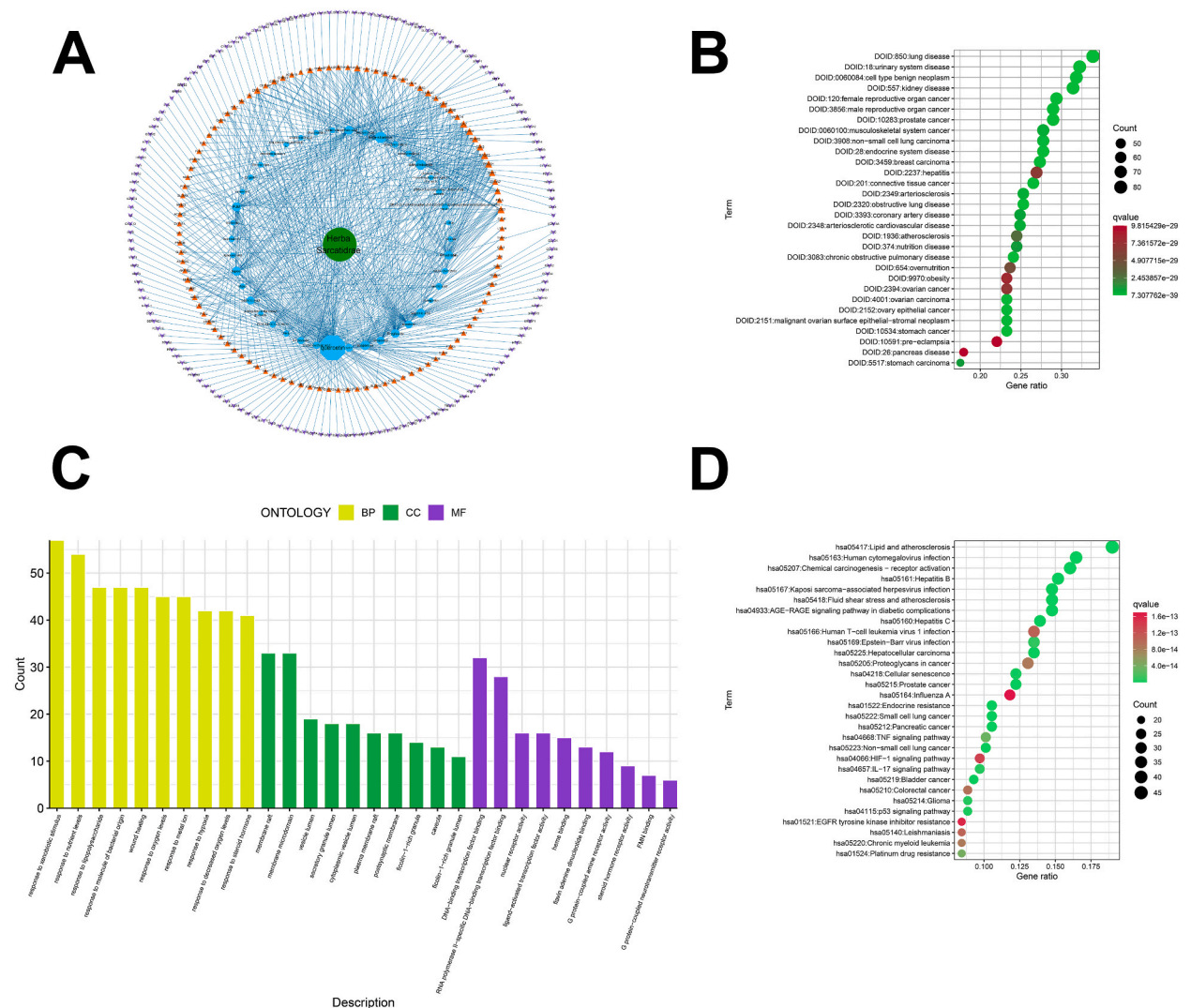
Fig. 1. Composition-target network of *herba sarcandrae*. (A) Regulatory network of *herba sarcandrae*-active ingredient-targets generated using Cytoscape (https://cytoscape.org/; ver. 3.7.2). (B) Disease Ontology (DO) analysis of the diseases associated with the targets of *the* active ingredients of herba sarcandrae. (C) Gene Ontology (GO) analysis of the biological processes, molecular functions, and cellular components related to the targets of *the* active ingredients of herba sarcandrae. (D) Kyoto Encyclopedia of Genes and Genomes (KEGG) enrichment analysis of the signaling pathways enriched by the potential targets of *the* active ingredients of herba sarcandrae.
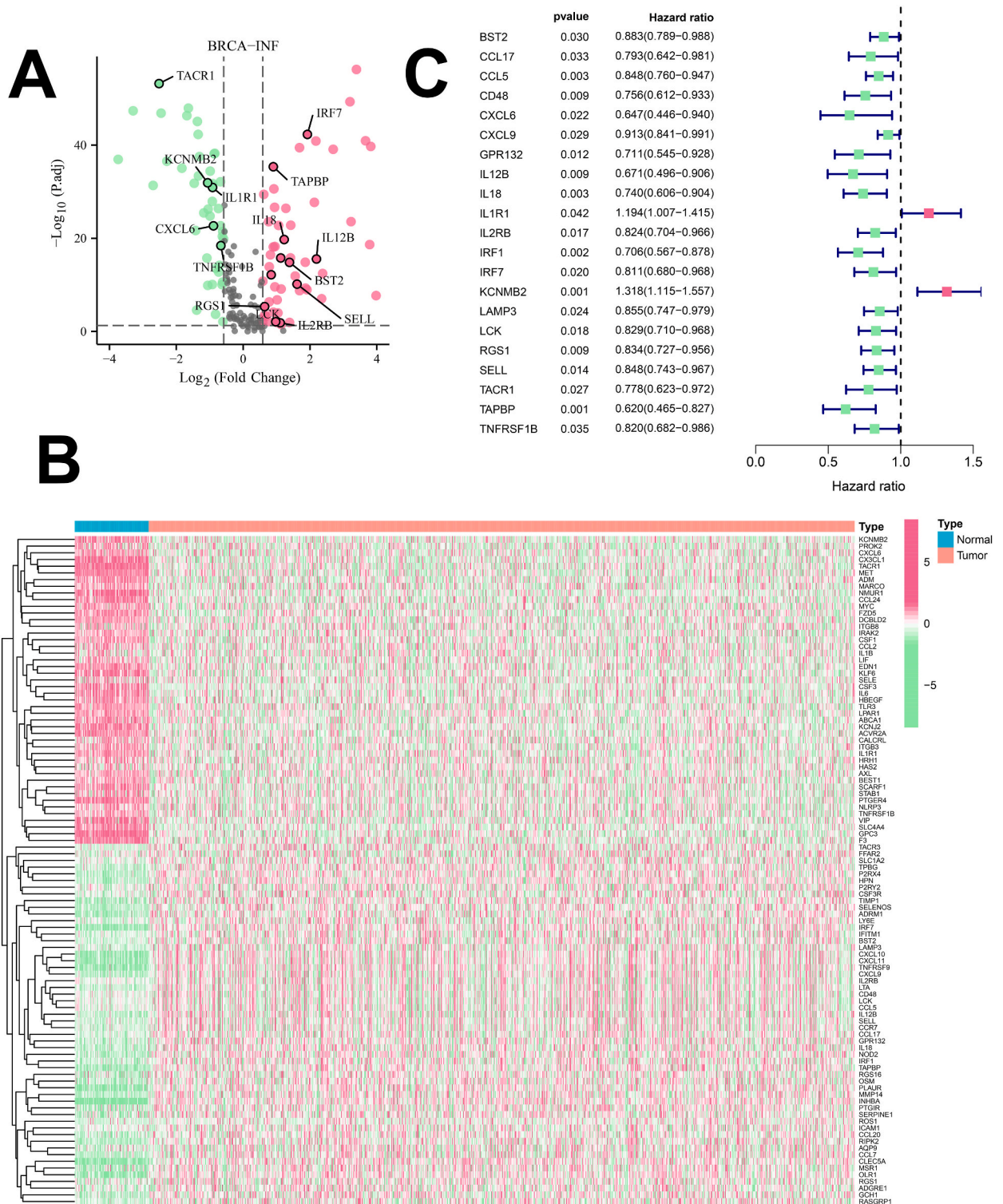
Fig. 2. Identification and annotation of DEGs associated with the inflammatory response in breast cancer (BRCA) (A) Volcano plot of DEGs related to the inflammatory response in BRCA based on data from The Cancer Genome Atlas (TCGA). (B) Heatmap of DEGs related to the inflammatory response in BRCA. Blue represents the normal sample; pink represents the tumor sample. (C) Forest plots from univariate Cox regression analysis of TCGA data.

2.11. Tumor-bearing nude mouse model construction

Briefly, 15 female BALB/C nude mice (3–4 weeks old) (Gempharmatech, Jiangsu, China) were utilized (5 mice/group). The 4T1 cell suspension (100 μL, 5×10^7/mL) was subcutaneously implanted in the right armpit of nude mice. After tumorigenesis (0.5–0.7 cm^3), the mice were administered Zhongjiefeng (STATE MEDICAL PERMITMENT No. Z20090321, 5 mg/kg, gavage, once a day) and rutin (500 mg/kg, intraperitoneal injection, once a day). Tumor size was calculated by the following formula: volume (mm^3) = length $\times$ width^2/2. Twenty days later, the tumors were removed after the animals had been euthanized, followed by measurement of the tumor weight and processing of the tumor tissues for subsequent analyses. The study was approved by the Ethics Committee of Guangzhou Forevergen Medical Laboratory Animal Center (approval number IACUC-AEWC-F2303012).

2.12. Immunohistochemical (IHC) analysis

The excised tumor samples were embedded and fixed. Sections were microwaved in Retrieval Solution (Amyjet, Wuhan, China) at pH 6.0 or pH 9.0 for 7 min, followed by incubation in 3 % H_2O_2 for 10 min. Nonspecifically bound sites were then blocked with 2.5 % normal horse serum (Vector Biolabs, Burlingame, CA, USA). The sections were incubated with an antibody against Ki67 (#ab279653, Abcam, USA). After incubation with a secondary antibody (#ab125913, Abcam) for 30 min, the sections were stained with 3,3′-diaminobenzidine solution (Sangon Biotech, Shanghai, China) and hematoxylin (Sangon Biotech). Representative areas were viewed under a light microscope (Nikon 90i, Tokyo, Japan).

2.13. Immunofluorescence (IF)

The sections were routinely dewaxed and hydrated, followed by the addition of 3 % H_2O_2 to remove endogenous oxidative enzymes. After antigen retrieval by boiling in 0.01 M sodium citrate buffer solution (pH 6.0) (Sangon Biotech) and sealing with 5 % BSA, sections (5 μM) were incubated overnight with antibodies against CD4 (#A0363, 1:1000, ABclonal), CD8 (#A11856, 1:1000, ABclonal), or PD-L1 (#A1645, 1:1000, ABclonal) at 4 °C. After washing with PBS three times, the sections were incubated for 2 h with a secondary antibody (ZF-0516/ZF-0512, Zhongshan Jinqiao Technology Co., Ltd., Beijing, China). After staining with 4',6-diamino-2-phenylindole (DAPI), the results were observed using a fluorescence microscope (M152-N, Mingmei, Shandong, China).

2.14. Statistical analysis

The experimental data were analyzed using GraphPad Prism 8.0. The values from three independent experiments are presented as the mean $\pm$ standard deviation (SD). Significant differences between the two groups were identified by t-tests. Comparisons involving multiple groups were performed using a one-way analysis of variance (ANOVA). A criterion of $p < 0.05$ was established for statistical significance.

3. Results

3.1. Corresponding targets of the active ingredients of herba sarcandrae

To investigate the relationship between the active ingredients of *herba sarcandrae* and the corresponding targets in BRCA, the regulatory network of *herba sarcandrae*-active ingredient targets was first explored through multiple databases. Briefly, the relevant targets of the active ingredient of *herba sarcandrae* were retrieved through multiple drug-related databases, such as SymMap, TCMID, and TCMSP, and the gene names of the matching targets were corrected via the UniProt database (https://www.uniprot.org/). A total of 41 active ingredients of *herba sarcandrae* were identified, and 265 potential targets of these active ingredients were identified. A protein-protein interaction (PPI) network of *herba sarcandrae*-active ingredient-targets was constructed with the help of Cytoscape 3.7.2 software (Fig. 1A). We then conducted DO/GO/KEGG enrichment analysis on potential targets of *herba sarcandrae* active ingredients. DO analysis found that a total of 67 genes were enriched in BRCA, including RELA/CCNA2/ESR1/PTGS2/PPARG/MAPK14/GSK3B/CCND1/ESR2 (Fig. 1B). The potential targets of *herba sarcandrae* active ingredients were mainly enriched in response to xenobiotic stimulus, response to nutrient levels, and so on (Fig. 1C). KEGG analysis presented that the potential active ingredient targets of *herba sarcandrae* were mainly enriched in the AGE-RAGE signaling pathway in diabetic complications, lipid and atherosclerosis, fluid shear stress and atherosclerosis, and other pathways (Fig. 1D).

3.2. DEGs related to the inflammatory response in BRCA

To analyze breast cancer-associated inflammatory genes, we downloaded clinical transcriptome expression data associated with BRCA from the TCGA database and used the R software "limma" package to collate and summarize the downloaded data to further derive the expression matrix associated with the inflammatory response (a total of 200 inflammatory response-associated genes were included). DEGs related to the inflammatory response in BRCA were screened (FDR value < 0.05, $|\log_2 FC| \geq 0.585$). Fifty-five upregulated mRNAs and 46 downregulated mRNAs were screened, and volcano heatmaps and expression matrix heatmaps of these DEGs were generated, as shown in Fig. 2A and B. In addition, we conducted univariate analysis on these DEGs and found that high expression of IL1R1 and KCNMB2, as well as low expression of BST2, CCL17, CCL5, CD48, CXCL6, CXCL9, GPR132, IL12B, and IL18,

was strongly linked to BRCA prognosis (Fig. 2C). The aforementioned group of inflammatory response genes that affect outcomes for BRCA patients was used for survival prognosis analysis using TCGA-BRCA or GEO-BRCA clinical data. The results showed that the BST2, CXCL6, GPR132, IL12B, IL18, IL1R1, IL2RB, IRF1, IRF7, KCNMB2, LCK, RGS1, SELL, TACR1, TAPBP, and TNFRSF1B genes had significant impacts on the survival and prognosis of patients with BRCA (Fig. S1A-P). Among them, BRCA patients with high expression
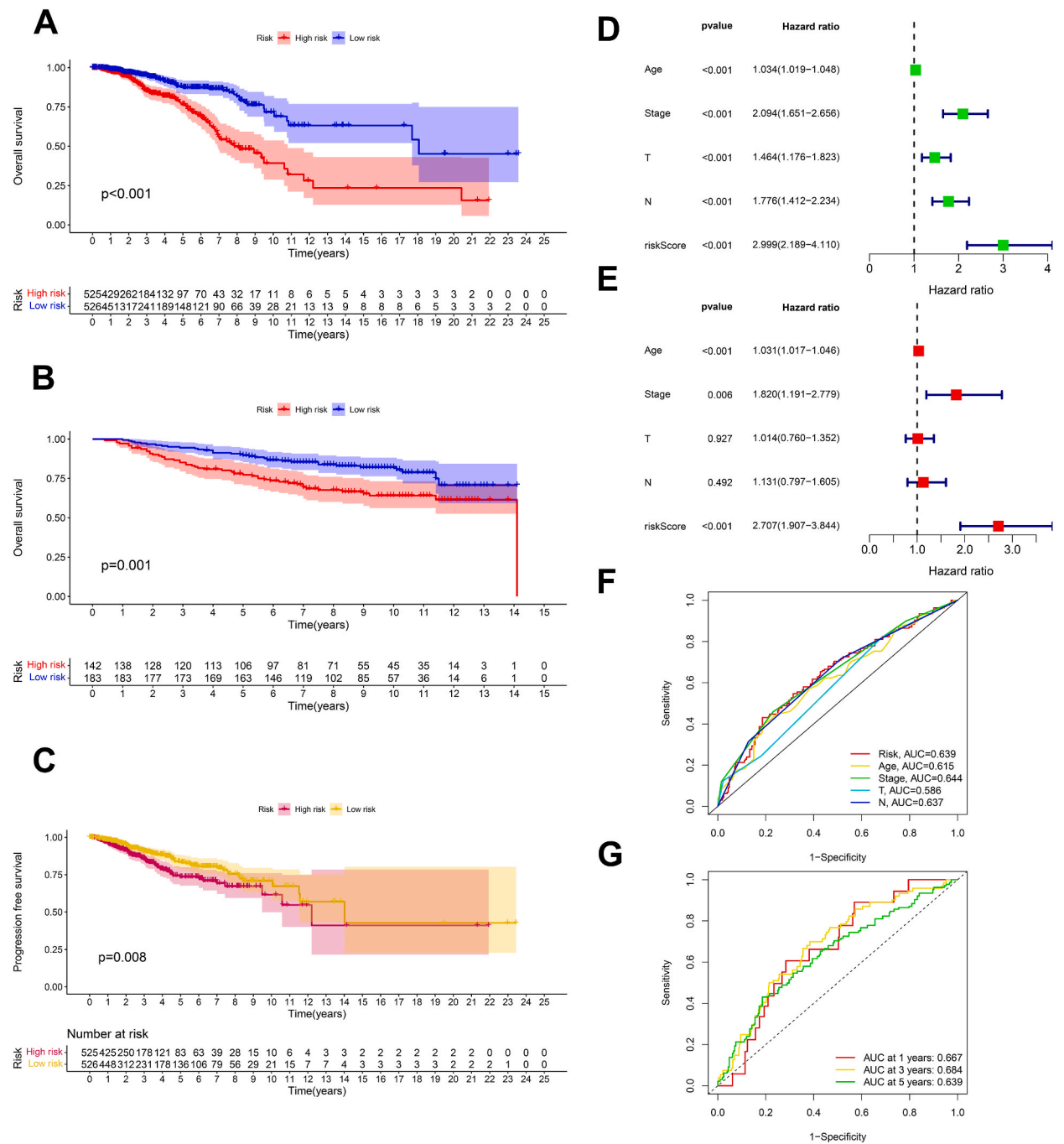

Fig. 3. Construction and validation of a BRCA inflammatory response-related risk scoring model. (A–B) OS of patients in the TCGA-BRCA (A) and GEO-BRCA (B) cohorts. (C) PFS of patients in the TCGA-BRCA cohort. (D–E) Univariate (D) and multivariate (E) analyses were conducted using the 16-INF gene signature and clinical covariates based on overall survival in the TCGA-BRCA cohort. (F) ROC analysis of the specificity and sensitivity of prognosis prediction by the 16-interferon (INF) gene risk score, age, T and N classifications, and tumor stage in the TCGA-BRCA cohort in terms of overall survival. (G) Validation of the prognostic value of the survival-dependent receiver operating characteristic (ROS) curve at 1, 2, and 3 years in the TCGA cohort.

of BST2, CXCL6, GPR132, IL12B, IL18, IL2RB, IRF1, IRF7, LCK, RGS1, SELL, TACR1, TAPBP, or TNFRSF1B had a better prognosis than those with low expression of these genes. In contrast, BRCA patients with higher expression of IL1R1 or KCNMB2 had a worse prognosis.

3.3. Construction of risk score models associated with the BRCA inflammatory response

To explore the association of immune-inflammation-related DEGs with survival, we constructed prognostic models for the above 16 INF genes. According to the risk score, all patients in the TCGA cohort were clustered into high-risk (525 patients) and low-risk (526 patients) groups, and survival was significantly lower in BRCA patients in the high-risk subgroup (Fig. 3A). Similarly, overall survival was significantly reduced in BRCA patients in the high-risk group according to the GEO database (Fig. 3B). However, patients suffering from BRCA within the high-risk group had considerably shorter survival than those within the low-risk group (Fig. 3C). Univariate Cox regression model analysis revealed that age, tumor stage, T and N classification, and risk score may influence overall survival in patients with BRCA (Fig. 3D). The factors that may affect the prognosis of patients with BRCA were incorporated into a multivariate Cox regression model, and the results showed that age, tumor stage, and risk score were found to be independent prognostic factors for BRCA (Fig. 3E). Subsequently, we performed ROC analysis to evaluate the performance of a model containing 16 INF genes in predicting prognosis. The prognostic prediction of the 16-INF gene risk score model for BRCA patients had an AUC of 0.639, which was superior to that of age and T and N classifications (Fig. 3F). In addition, we constructed ROC curves for the 1-, 3-, and 5-year periods, and the results showed that the AUC of these three groups was greater than 0.6, suggesting that the model containing 16 INF genes had good accuracy in predicting survival rates within 3 years for BRCA patients (Fig. 3G).
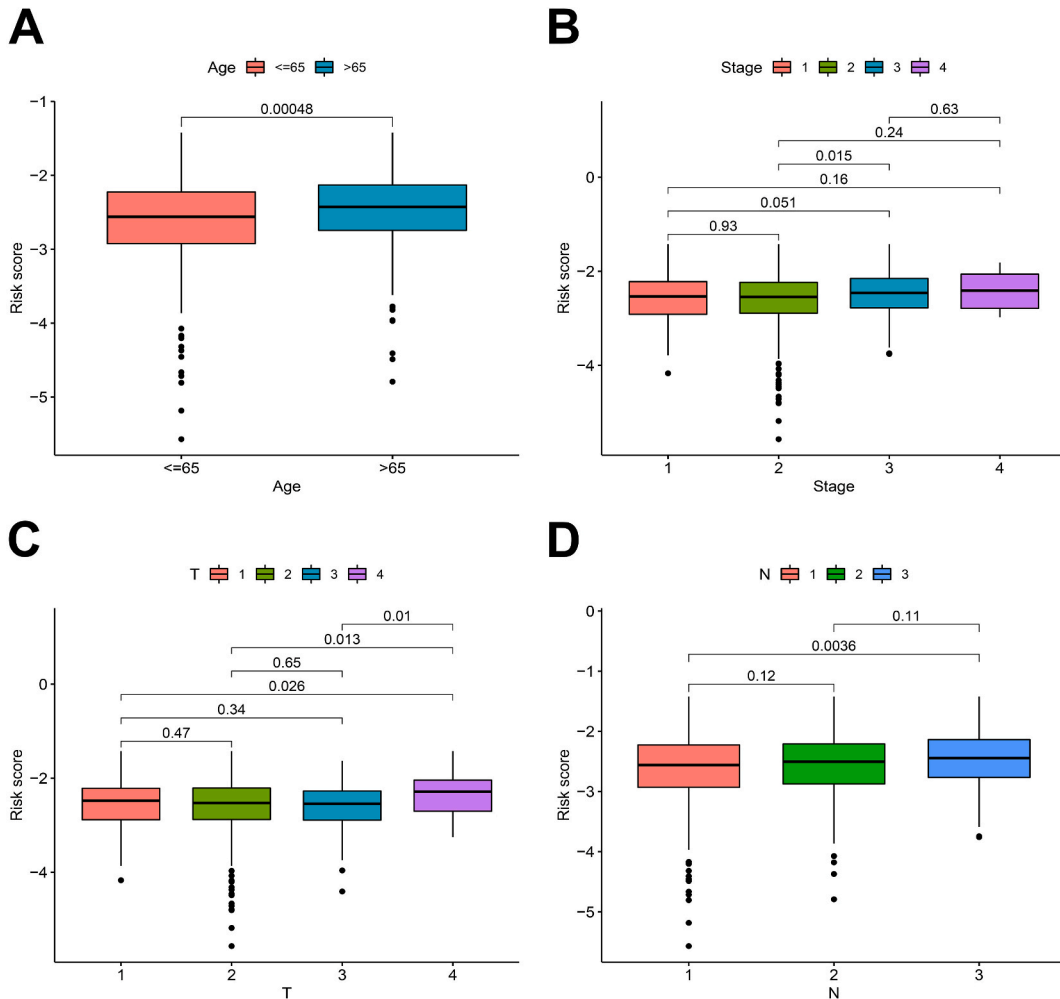
Fig. 4. Relationships between the risk model and clinical features. (A–D) Analysis of the relationships between the 16-INF gene risk score and clinical features such as age, T and N classifications, and tumor stage in the TCGA-BRCA cohort.
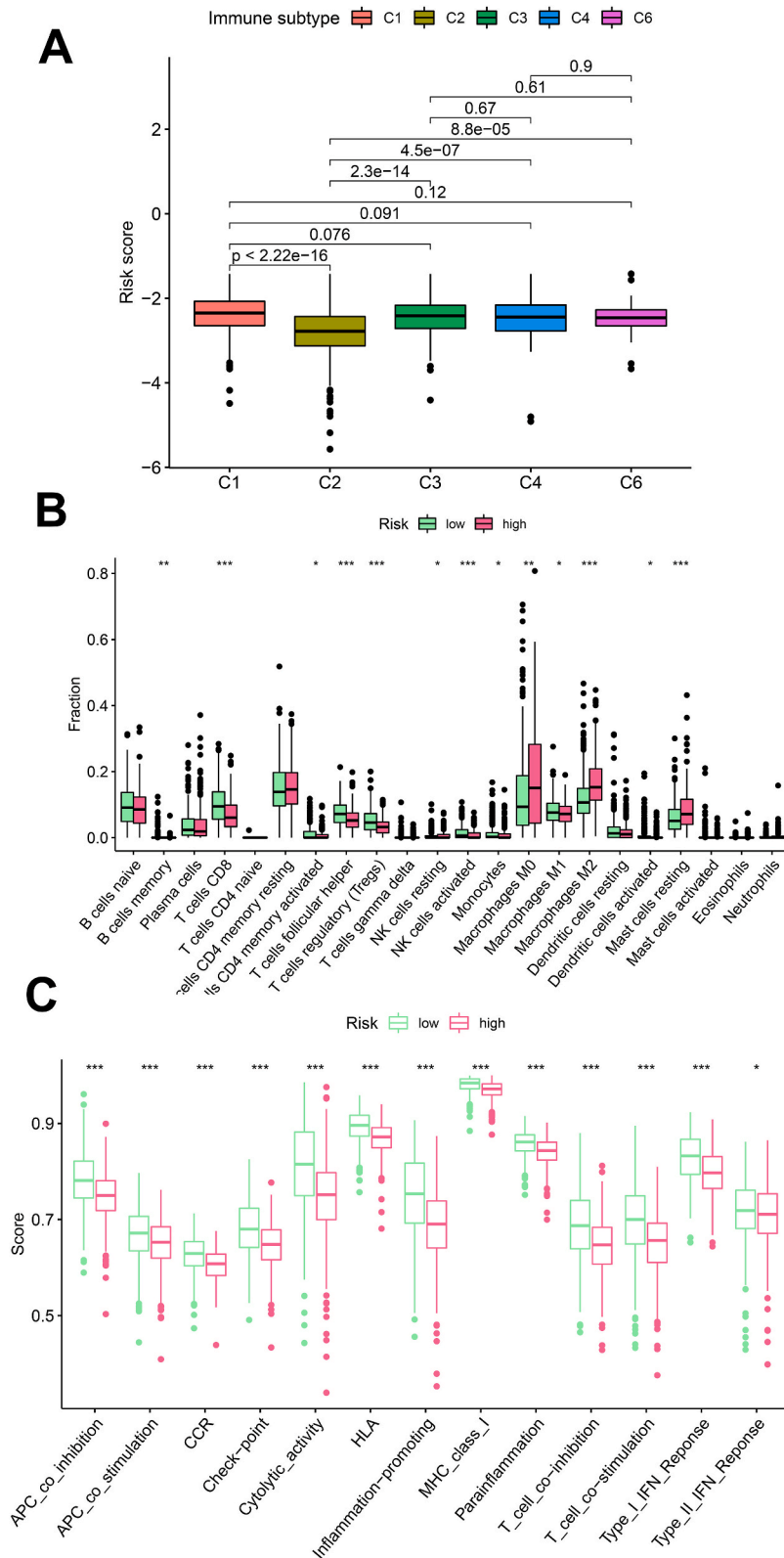
**Fig. 5. Relationships between the risk model and immune response.** (A) Analysis of the relationship between the 16-INF gene risk score and six types of infiltrating immune cells. (B) Analysis of the degree of immunocyte infiltration in the 22 immunocyte subunits in the high-risk and low-risk groups. (C) Differences in immune-related functions between the high- and low-risk groups. (*$p < 0.05$; **$p < 0.01$; ***$p < 0.001$).

3.4. Correlations of the risk score models with clinical features and immune cell functions

To investigate whether this risk model is associated with the clinical features of patients with BRCA, the Wilcoxon rank sum test was carried out. BRCA patients with older age, later TNM stage, and higher tumor grade were observed in the high-risk group (Fig. 4A–D). The function of the 16-INF gene (overexpression) risk model in the immune response was described. The correlation between the risk score and infiltrating immune cells was analyzed, and the results showed that the 16-INF gene (overexpression) risk model did not significantly differ among the six types of immune infiltration, but it was mainly enriched in the C1 and C3 subtypes (Fig. 5A). The study inferred the proportion of immune cells in 22 types of infiltrating immune cells from standardized gene expression data using the CIBERSORT algorithm with 1000 permutations. The low-risk group had higher proportions of T cells CD8$^+$, B-cell memory, activated T cells CD4$^+$ memory, T cells follicular helper, regulatory T cells, activated NK cells, monocytes, and M1 macrophages than did the high-risk group, but the high-risk group had significantly greater proportions of M2 macrophages, resting NK cells, M0 macrophages, and resting mast cells than did the low-risk group (Fig. 5B). Moreover, its immune functions were mainly concentrated in check-point, cytolytic_activity, APC_co_inhibition, MHC_class_I, APC_co_stimulation, CCR, HLA, inflammation-promoting, and so on (Fig. 5C).

3.5. GO and KEGG enrichment analyses of prognostic risk genes

To determine the relevance of the BRCA inflammatory response gene cluster to immune cell function, the Bioconductor package and clusterProfiler package in R were used to perform GO analysis and KEGG pathway enrichment analysis of 16 INF genes and DEGs associated with prognostic risk genes. GO analysis revealed that the enriched biological processes of these genes included positive regulation of leukocyte activation, positive regulation of cell activation, and immunoglobulin production. The components were mainly enriched in circulating, immunoglobulin complex, immunoglobulin complex, and the external side of the plasma membrane. The enriched molecular functions included C–C chemokine binding, immunoglobulin receptor binding, and antigen binding. Furthermore, they focused mainly on the T-cell receptor signaling pathway, Th17 cell differentiation, viral protein interaction with
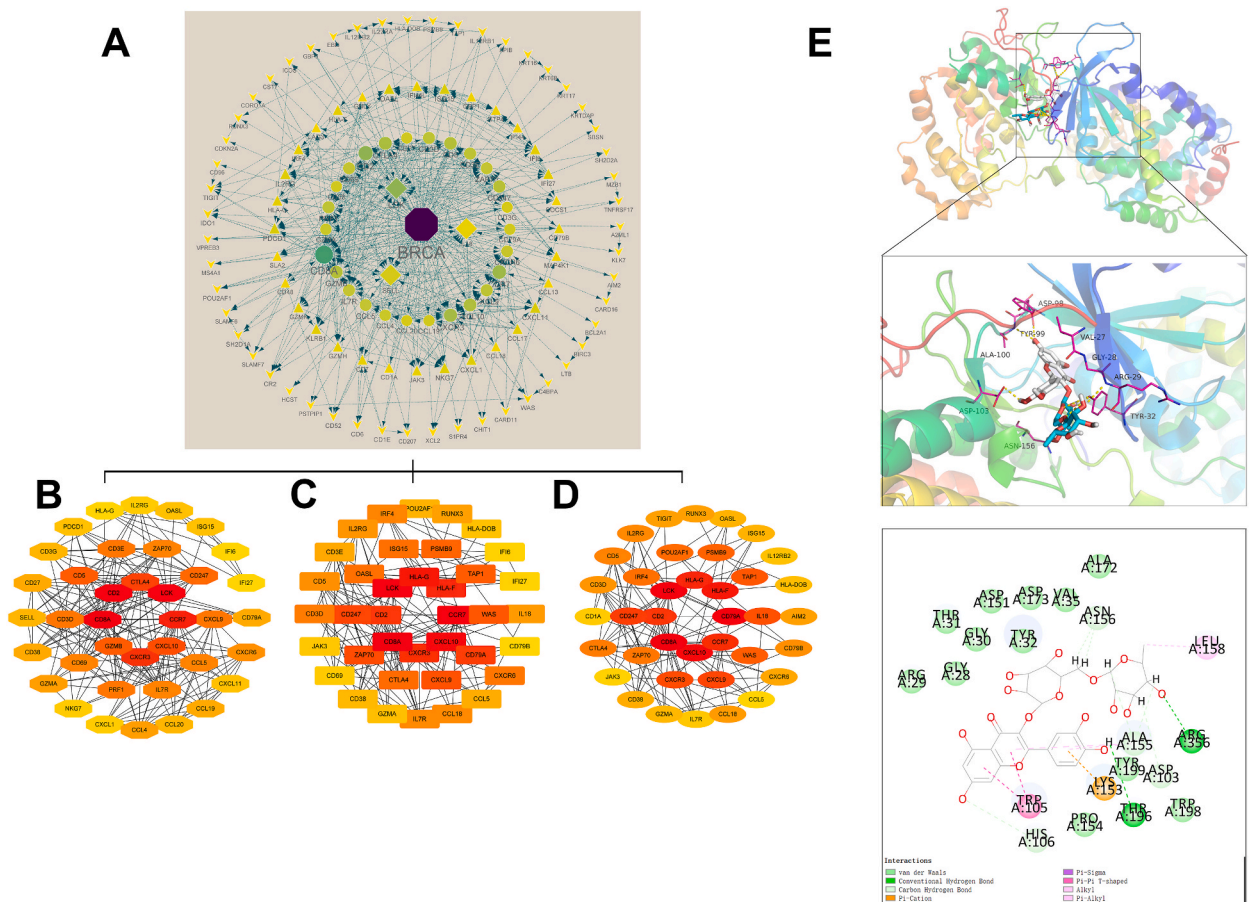

Fig. 6. The core gene network of inflammation genes related to BRCA. (A) The core targets of PPIs. (B) The distribution network of degree core targets. (C) The distribution network of stress core targets. (D) The distribution network of betweenness core targets. (E) Molecular docking results of the core protein IRF1 with the active compound rutin.

cytokine and cytokine receptors, hematopoietic cell lineage, primary immunodeficiency, cytokine–cytokine receptor interaction, and other pathways. In addition, we performed PPI and topology analyses, the network diagram of which is shown in Fig. 6A–D.

3.6. Core protein screening and molecular docking

To screen the most core drug-sensitive proteins, the 41 active ingredients of *herba sarcandrae* mined from the results were molecularly docked to identify potential drugs targeting the core protein IRF1 (mutual mapping and matching between herba sarcandrae targets and BRCA-INF prognostic risk genes). The pdb structure of the core protein IRF1 was downloaded from the PDB (PDB ID: 4CRL). We downloaded the sdf files of 41 active ingredients from the PubChem database and docked all of them with the core protein IRF1. Based on the LibDockScore (LibDockScore) values, we found that IRF1 might bind strongly to epimedin C, lignoceric acid, docosanoate, pelargonidin-3-rhamnosyl glucose, Engelitin, sitoglucide, beta-sitosterol, sitosterol, and rutin, suggesting that these compounds may be drugs that target IRF1. We further used AutoDock-Vina to dock drugs to more accurately identify drugs that bind to the IRF1 domain. Epimedin C, lignoceric acid, Docosanoate, pelargonidin-3-rhamnosyl glucoside, Engelitin, Sitogluside, beta-sitosterol, sitosterol, rutin, and 9 other active ingredients were selected as drug candidates for the IRF1 active site, and their affinities were ≤-5.0 kcal/mol. Additionally, the RMSD values were <2.00, except for those of rutin and the core protein IRF1, indicating that the docking model was reliable. Combining the LibDock score, binding energy, and RMSD values, the docking complex formed by
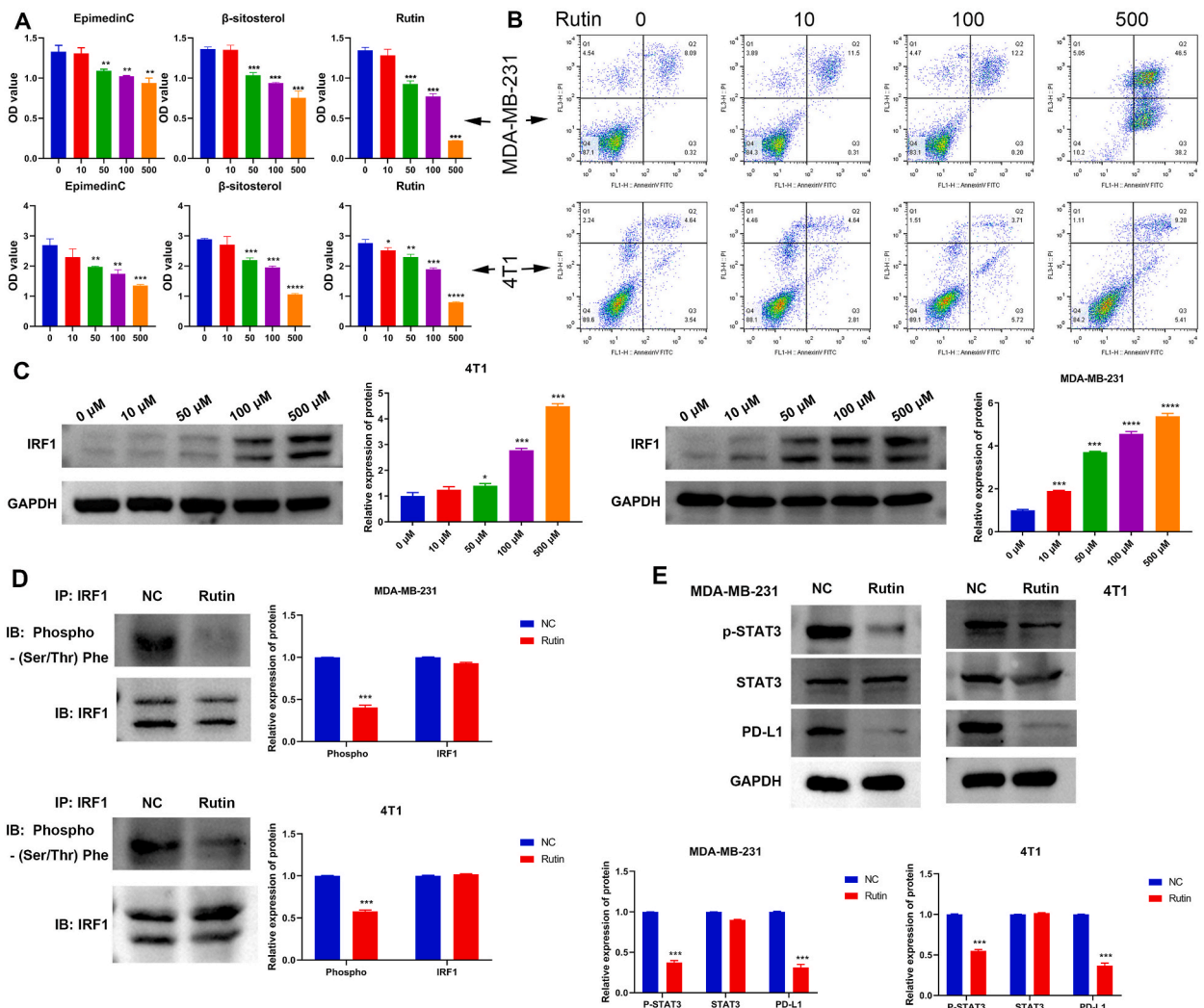
Fig. 7. Effects of rutin on proliferation, apoptosis, and the IRF1/STAT3/PD-L1 pathway in BRCA cells. (A) CCK-8 analysis of the effects of different concentrations of epimedin C, rutin, or β-sitosterol (0, 10, 50, 100, 500 μM) on BRCA cell viability. (B) Flow cytometry analysis of the effect of rutin (50 μM) on the apoptosis of BRCA cells. (C) Mouse 4T1 and human MDA-231 cells were treated with 0, 10, 100, or 500 μM rutin for 48 h, and the protein level of IRF1 was detected by western blotting. Image was cropped. (D) Co-IP analysis of the interaction between rutin and IRF1. Image was cropped. (E) Western blot analysis of p-STAT3/STAT3/PD-L1 protein levels in MDA-MB-231 cells treated with or without rutin. Image was cropped. (*$p < 0.05$; **$p < 0.01$; ***$p < 0.001$).
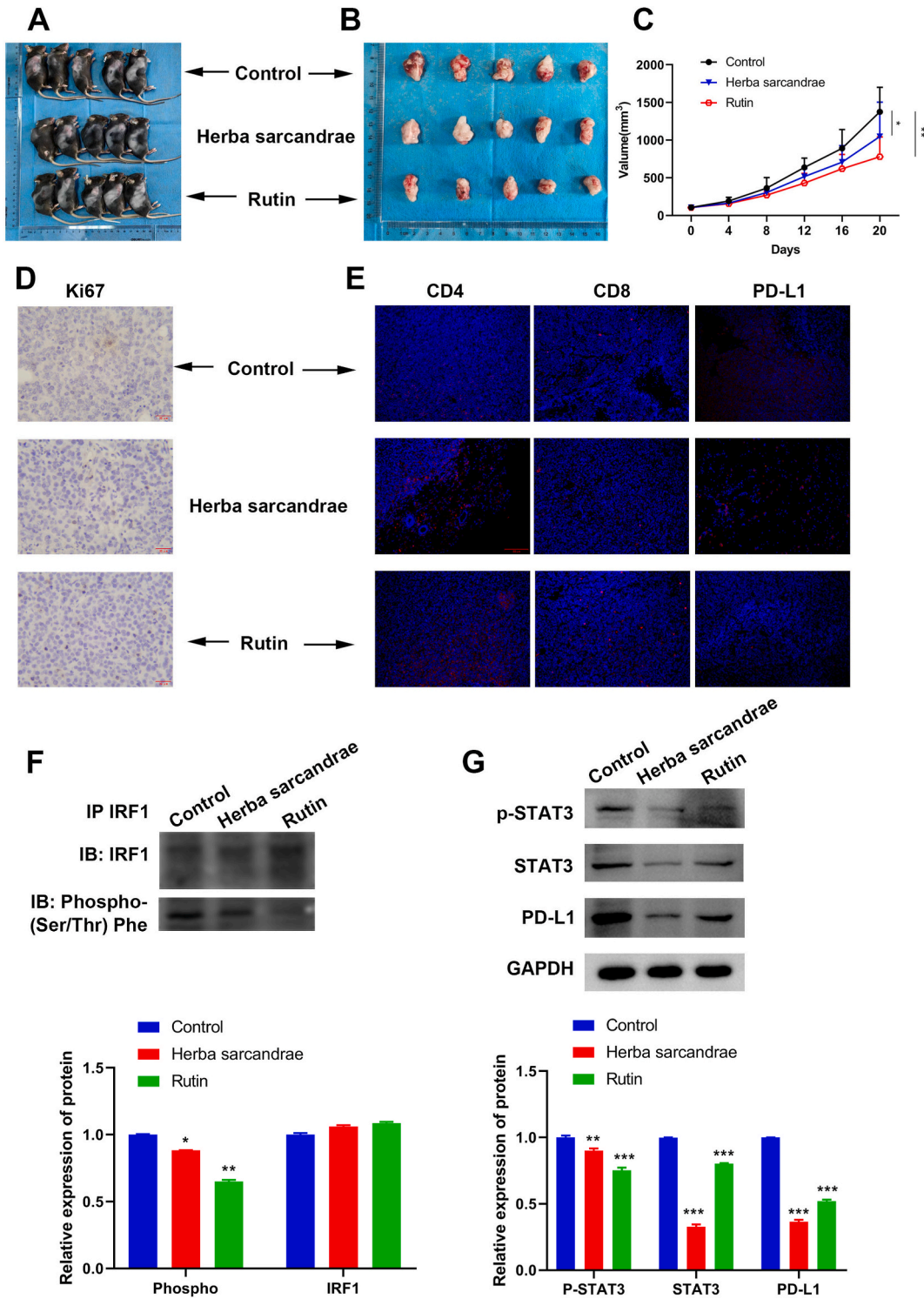
Fig. 8. Antitumor effects of *herba sarcandrae* and rutin in a nude mouse tumor model. (A and B) Representative images of nude tumor model mice and tumors from different groups (n = 5 per group). (C) Time course of tumor growth in each group at the indicated time points. (D) Representative Ki-67 staining of tumors from different groups. (E) IF detection of CD4, CD8, and PD-L1 protein levels in tumors from different groups. (F) Co-IP analysis of the interaction between *herba sarcandrae* or rutin and IRF1. Image was cropped. (G) Protein levels of p-STAT3, STAT3, and PD-L1 in tumors from different groups. Image was cropped. (*$p < 0.05$; **$p < 0.01$; ***$p < 0.001$).

Sitogluside and the core protein IRF1 was the best (Fig. 6E). Therefore, the above 9 active ingredients may be used as drugs that target the IRF1 protein.

3.7. Rutin mediated proliferation, apoptosis and the IRF1/STAT3/PD-L1 pathway in BRCA cells

To analyze the effects of the traditional Chinese medicine monomers epimedin C, rutin, and β-sitosterol on BRCA cell lines, we treated BRCA cells with concentrations of sitogluside, epimedin C, rutin, and β-sitosterol (0, 10, 50, 100, 500 μM) for 48 h, respectively. The CCK-8 assay results also showed that the effect of Sitogluside treatment was not very significant (Fig. S2). CCK-8 assays further showed that the monomers epimedin C, rutin, and β-sitosterol at concentrations greater than or equal to 50 μM could significantly repress the activity of BRCA cells, and rutin could inhibit BRCA cell activity at a concentration of 10 μM (Fig. 7A). Subsequently, rutin was selected for further analysis. Moreover, rutin facilitated BRCA cell apoptosis in a concentration-dependent manner (Fig. 7B). Western blotting data showed that rutin markedly upregulated IRF1 in mouse 4T1 and human MDA-231 cells, and the expression level of IRF1 gradually increased with increasing rutin concentration (Fig. 7C). Co-IP revealed that rutin (50 μM) weakened the phosphorylation of Phe in BRCA cells (Fig. 7D). We further analyzed the effect of rutin on the expression of the immune-associated genes STAT3, p-STAT3, and PD-L1, which are located downstream of IRF1. Western blotting revealed that rutin markedly reduced p-STAT3 and PD-L1 protein levels in BRCA cells (Fig. 7E). Overall, rutin mediated proliferation, apoptosis, and the IRF1/STAT3/PD-L1 pathway in BRCA cells.

3.8. Herba sarcandrae and rutin decreased tumor growth in a nude mouse tumorigenic model

To investigate the effect of *herba sarcandrae* and rutin on BRCA growth *in vivo*, we constructed a nude mouse tumorigenesis model with 4T1 cells. The results showed that the size of the tumors formed by 4T1 cells was smaller in the *herba sarcandrae* and rutin groups than in the control group (Fig. 8A–C). IHC staining revealed fewer ki67-positive cells in tumor samples from the *herba sarcandrae* and rutin groups than in tumor samples from the control group (Fig. 8D). IF staining revealed an increase in CD4 and CD8 expression and a decrease in PD-L1 expression in tumor samples derived from SMN- and rutin-treated mice (Fig. 8E). Furthermore, *herba sarcandrae* and rutin treatment decreased the level of IRF1 protein phosphorylation in mouse tumors, as evidenced by co-IP (Fig. 8F). In addition, *herba sarcandrae* and rutin treatment decreased p-STAT3, STAT3, and PD-L1 protein levels in mouse tumors (Fig. 8G). Overall, *herba sarcandrae* and rutin decreased BRCA growth in a nude mouse tumorigenic model by blocking the IRF1/STAT3/PD-L1 pathway.

4. Discussion

Molecular docking is a theoretical simulation method that mainly studies the interactions between molecules and predicts their binding mode and affinity [18]. This approach plays a crucial role in the field of computer-aided drug research. The principle of spatial matching and energy matching aims to find the best combination of drug molecules and biological molecules to understand the mechanism of action of drugs [19]. In cancer research, molecular docking helps to discover new anticancer drugs or drug candidates, and the therapeutic effect of drugs on cancer can be predicted by simulating the interaction between drugs and cancer-related target proteins. Network pharmacology is an emerging method that combines computer science and medicine to explain the mechanism of action of drugs on diseases [20]. This method can be used to systematically study and identify bioactive compounds in traditional Chinese medicine formulations and visualize their multi-target and multi-pathway mechanisms [21]. In cancer research, network pharmacology is helpful for comprehensively understanding the role of drugs in complex biological systems and for predicting and analyzing the pharmacological effects and potential mechanisms of drugs [22]. Combining these two technologies gives full play to their advantages [23]. Molecular docking can provide detailed molecular interaction data for network pharmacology to more accurately construct interaction networks between drugs and cancer-related target proteins. Network pharmacology can analyze these interactions at the system level and reveal the multitarget and multi-pathway mechanisms of the action of drugs in cancer treatment. This combination helps to discover new anticancer drugs, optimize the therapeutic effect of existing drugs, and provide strong support for personalized cancer treatment. The combination of these two techniques has been used in multiple cancer studies, such as studies on colorectal cancer [24], leukemia [25], lung cancer [26], osteosarcoma [27], and breast cancer [28].

Many studies have shown that the volatile oil and extract of *herba sarcandrae* have certain inhibitory effects on cancer cells, such as leukemia and lung cancer cells [8]. In addition, the total flavonoid glycoside of *herba sarcandrae* also has a strong killing effect on Aili ascites-derived cancer cells *in vitro*, and the inhibition rate of cancer cells after intraperitoneal administration can reach 70.8 % [29]. These findings suggest that *herba sarcandrae* may play a vital role in cancer treatment, helping to slow the growth of tumor cells and improve the quality of life of cancer patients. In this study, the network of the "component-target-disease-pathway" pathway in the *herba Sarcandrae* was fully characterized through integrated pharmacological methods. Subsequently, by analyzing high-throughput data, DEGs related to inflammation were screened from the BRCA-TCGA database, and biomarkers and risk prediction genes related to BRCA inflammation were identified. Finally, molecular docking technology predicted the affinity between small drug molecules and targets, revealing the interactions between drug molecules and targets, elucidating their structure-activity relationships and validating the *herba Sarcandrae*'s ability to modulate the immunosuppression of the BRCA process through IRF in breast cancer cells and tumor animal models.

The research and development model of network pharmacology based on multiple components and multiple targets is more in line with the complex and diverse components and pharmacological effects of TCM. This study identified a total of 41 active drug molecules of *herba sarcandrae* and predicted 265 therapeutic targets for *herba sarcandrae* through integrated pharmacological methods. DO

analysis revealed that a total of 67 genes were enriched in BRCA among 265 potential targets, including RELA, CCNA2, ESR1, PTGS2, PPARG, MAPK14, GSK3B, CCND1, and ESR2. GO analysis revealed that 265 potential targets were mainly enriched in response to xenobiotic stimuli, response to oxygen levels, response to molecules of bacterial origin, response to lipopolysaccharide, response to nutrient levels, etc. Moreover, 265 potential targets were mainly enriched in pathways such as the AGE-RAGE signaling pathway in diabetic applications and chemical carcinogenesis receptor activation. These results indicated that *herba sarcandrae* could be used for the clinical treatment of tumors, metabolic diseases, and inflammatory diseases, which was consistent with modern research results and in line with the application experience of *herba sarcandrae* [8,30]. These results indicated that the multitarget drug *herbsa sarcandrae* can simultaneously stimulate multiple targets in the disease signaling pathway, providing a new avenue for BRCA clinical treatment.

In this study, 101 DEGs associated with BRCA inflammation, including 55 upregulated genes and 46 downregulated genes, were identified by analyzing TCGA-BRCA data. Univariate analysis and bioinformatics analysis revealed that the effects of the BST2 [31], CXCL6 [32], GPR132 [33], IL12B [34], IL18 [35], IL1R1 [36], IL2RB [37], IRF1 [38], IRF7 [39], KCNMB2 [40], LCK [41], RGS1 [42], SELL, TACR1, TAPBP and TNFRSF1B [43] genes on the prognosis of patients with BRCA were significant, and a search of the literature revealed that some of the 16 genes are therapeutic targets and risk predictors for BRCA [44,45]. A prognostic model for the 16 inflammatory genes was constructed, and the predictive ability of this prognostic model was verified, highlighting the prognostic survival curves and plots containing 16 gene signatures and clinicopathological parameters showing great prognostic efficacy, which might allow clinicians to make judgments about outcomes for individual patients. Overall, high expression of IL1R1 and KCNMB2 and low expression of BST2, CCL17, CCL5, CD48, CXCL6, CXCL9, GPR132, IL12B, and IL18 are related to BRCA patient survival and prognosis. However, subsequent experimental verification of these genes is still needed to identify potential clinical therapeutic targets.

We also conducted a functional analysis of 16 gene signatures. These genes were mainly related to biological processes such as positive regulation of leukocyte activation, positive regulation of cell activation, and immunoglobulin production. These pathways were mainly related to cytokine receptor interactions, lineage, primary immunity, and hematopoietic cell viral protein interactions with cytokines and cytokine receptors. Through the above results, we easily found that the prognostic model was mainly related to the immune response, as inflammation is significantly associated with the human immune response [46]. TILs are a mixture of proinflammatory immune cells and immunosuppressive cells [47]. Interstitial TILs are more important for the prognosis of patients with BRCA, as they are not affected by tumor nest density or growth patterns [48]. TILs can clear tumor cells, recognize tumor antigens, and induce antitumor immune responses [49]. High levels of TILs can predict favorable prognosis for BRCA patients [50] and are strongly associated with high pathological complete response rates in BRCA patients receiving neoadjuvant therapy [51,52]. This study analyzed the effect of this prognostic model on TILs. Analysis confirmed that low-risk patients often had greater numbers of TILs and stronger immune pathway activity. High levels of TILs suggest that patients have a better prognosis [50], so the low-risk group in this model has a better prognosis.

IRF1 is the most important transcription factor in the interferon (IFN) pathway. IRF1 is induced by type I IFN (IFN-α, IFN-β), type II IFN (IFN-γ), IL-1, IL-6, and TNF-α [53]. IRF1, a transcription factor, can activate a series of target genes, stimulate the production of inflammatory factors, promote immune cell differentiation and maturation, inhibit cell proliferation, and induce cell apoptosis. IRF1 plays an essential role during the EMT process in BRCA [38]. Several studies have associated the transcription factor IRF1 with tumor-suppressive activities [54,55]. SPOP mutants are deprived of the capability to degrade IRF1 and upregulate PD-L1 expression, thus accelerating tumor immune escape in endometrial cancer [56]. $CD8^+$ T cells in IRF1-deficient tumors suppress enhanced cytotoxicity *in vivo*. Tumor cells lacking IRF1 lose the ability to upregulate PD-L1 expression both *in vivo* and *in vitro* and are more susceptible to T-cell-mediated killing [54]. PD-L1 is upregulated in many cancers due to exogenous cellular stress. Studies have shown that PD-L1 is upregulated by STAT and IRF1 signaling in response to DNA double-strand breaks (DSBSs) [55]. This study conducted molecular docking on 41 active components of *herba sarcandrae* and identified 9 active components, namely, epimedin C, lignoceric acid, docosanoate, pelargonidin-3-rhamnosyl glucoside, Engelitin, sitoglucide, beta-sitosterol, sitosterol, and rutin, as candidate drugs targeting IRF1. Functionally, the monomers epimedin C, rutin, and β-sitosterol inhibited the activity of BRCA cells in a concentration-dependent manner. Subsequently, rutin was selected for further analysis. Moreover, rutin also promoted the apoptosis of BRCA cells in a concentration-dependent manner. Tumorigenesis in nude mice verified the tumor-inhibiting effect of *herba sarcandrae* and *rutin on* BRCA. Moreover, rutin weakened the phosphorylation of Phe in BRCA cells. Whether the docking site of the active ingredient of *herba sarcandrea* on IRF1 is the key site of the downstream cascade of phosphorylation remains to be further proven. In addition, rutin reduced p-STAT3 and PD-L1 protein levels in BRCA cells and subcutaneous tumors. These results showed that *herba sarcandrae* and *rutin* mediated cell proliferation and apoptosis via the IRF1/STAT3/PD-L1 pathway in BRCA.

The novelty of this study was that it was the first to explore and verify the mechanism of action of *herba sarcandrae* in the treatment of BRCA using emerging network pharmacology and that the potential of a 16-level inflammatory signature to predict prognosis in patients with BRCA has also been identified. In addition, the disadvantage of this study was that the different molecular types of BRCA had not been studied, which could be further analyzed in the future.

In summary, based on network pharmacology and molecular docking, the inhibitory effects of *herba sarcandrae* and *rutin* on BRCA might be mediated by the IRF1/STAT3/PD-L1 pathway through the key target IRF-1. The 16-level inflammatory signature could serve as a novel biomarker for predicting BRCA patient prognosis, providing more accurate guidance for clinical treatment prognosis evaluation and having important reference value for individualized treatment selection. However, breast cancer contains multiple subtypes, and whether this study applies to other subtypes of breast cancer is a major limitation of this study.

Data availability

Data included in article/supp. material/referenced in article.

CRediT authorship contribution statement

Jie Yuan: Writing – review & editing, Writing – original draft, Validation, Project administration, Methodology, Investigation, Funding acquisition, Formal analysis, Data curation, Conceptualization. **Minxia Lin:** Writing – review & editing, Writing – original draft, Validation, Methodology, Investigation, Formal analysis, Data curation, Conceptualization. **Shaohua Yang:** Writing – review & editing, Visualization, Validation, Software, Resources, Methodology, Investigation, Data curation, Conceptualization. **Hao Yin:** Writing – review & editing, Visualization, Validation, Software, Resources, Methodology, Investigation, Data curation, Conceptualization. **Shaoyong Ouyang:** Writing – review & editing, Visualization, Validation, Software, Resources, Methodology, Investigation, Data curation, Conceptualization. **Hong Xie:** Writing – review & editing, Visualization, Validation, Software, Resources, Methodology, Investigation, Data curation, Conceptualization. **Hongmei Tang:** Writing – review & editing, Visualization, Validation, Software, Resources, Methodology, Investigation, Data curation, Conceptualization. **Xiaowei Ou:** Writing – review & editing, Visualization, Validation, Software, Resources, Methodology, Investigation, Data curation, Conceptualization. **Zhiqiang Zeng:** Writing – review & editing, Validation, Project administration, Methodology, Investigation, Formal analysis, Data curation, Conceptualization.

Declaration of competing interest

The authors declare that they have no known competing financial interests or personal relationships that could have appeared to influence the work reported in this paper.

Appendix A. Supplementary data

Supplementary data to this article can be found online at https://doi.org/10.1016/j.heliyon.2024.e31137.

References

[1] J. Zhuo, Y. Zhao, J. Han, H. Li, R. Hao, Y. Yang, et al., Expression value of Rab10 in breast cancer, Clin. Exp. Obstet. Gynecol. 50 (8) (2023), https://doi.org/10.31083/j.ceog5008169.

[2] D.A. Elmaghraby, AMAb Hamad, K.M. Alhunfoosh, H.R. Alturifi, M.A. Albahrani, A.A. Alshalla, et al., Exploration and Assessment of breast cancer awareness in the Saudi population: a cross-sectional study, Clin. Exp. Obstet. Gynecol. 50 (11) (2023), https://doi.org/10.31083/j.ceog5011245.

[3] N. Jokar, I. Velikyan, H. Ahmadzadehfar, S.J. Rekabpour, E. Jafari, H.H. Ting, et al., Theranostic approach in breast cancer: a treasured tailor for future oncology, Clin. Nucl. Med. 46 (8) (2021) e410–e420, https://doi.org/10.1097/rlu.0000000000003678.

[4] F. Lüönd, S. Tiede, G. Christofori, Breast cancer as an example of tumour heterogeneity and tumour cell plasticity during malignant progression, Br. J. Cancer 125 (2) (2021) 164–175, https://doi.org/10.1038/s41416-021-01328-7.

[5] A. Kawiak, Molecular research and treatment of breast cancer, Int. J. Mol. Sci. 23 (17) (2022), https://doi.org/10.3390/ijms23179617.

[6] C. Li, R. Wen, D. Liu, L. Yan, Q. Gong, H. Yu, Assessment of the potential of sarcandra glabra (thunb.) nakai. In treating ethanol-induced gastric ulcer in rats based on metabolomics and network analysis, Front. Pharmacol. 13 (2022) 810344, https://doi.org/10.3389/fphar.2022.810344.

[7] J.N. Chu, P. Krishnan, K.H. Lim, A comprehensive review on the chemical constituents, sesquiterpenoid biosynthesis and biological activities of Sarcandra glabra, Natural products and bioprospecting 13 (1) (2023) 53, https://doi.org/10.1007/s13659-023-00418-8.

[8] Y. Zeng, J. Liu, Q. Zhang, X. Qin, Z. Li, G. Sun, et al., The traditional uses, phytochemistry and pharmacology of sarcandra glabra (thunb.) nakai, a Chinese herb with potential for development: review, Front. Pharmacol. 12 (2021) 652926, https://doi.org/10.3389/fphar.2021.652926.

[9] H. Sun, X. Lu, X. Hu, Z. Chen, J. Zhu, L. Lu, Effect and mechanism of total flavonoids from sarcandrae herba on the apoptosis in human leukemia K562 cells, Pharmacol Clin Chin Mater Med 35 (2019) 54–57, https://doi.org/10.3389/fphar.2021.652926.

[10] J. Shen, X. Zhu, Z. Wu, Y. Shi, T. Wen, Uvangoletin, extracted from Sarcandra glabra, exerts anticancer activity by inducing autophagy and apoptosis and inhibiting invasion and migration on hepatocellular carcinoma cells, Phytomedicine : international journal of phytotherapy and phytopharmacology 94 (2022) 153793, https://doi.org/10.1016/j.phymed.2021.153793.

[11] H. Li, H.L. Zhuang, J.J. Lin, Y.F. Zhang, H. Huang, T. Luo, et al., [Effect of rosmarinic acid from Sarcandra glabra in inhibiting proliferation and migration and inducing apoptosis of MDA-MB-231 cells via regulation of expressions of Bcl-2 and Bax], Zhongguo Zhong yao za zhi = Zhongguo zhongyao zazhi = China journal of Chinese materia medica 43 (16) (2018) 3335–3340, https://doi.org/10.19540/j.cnki.cjcmm.20180508.001.

[12] W.Y. Li, L.C. Chiu, W.S. Lam, W.Y. Wong, Y.T. Chan, Y.P. Ho, et al., Ethyl acetate extract of Chinese medicinal herb Sarcandra glabra induces growth inhibition on human leukemic HL-60 cells, associated with cell cycle arrest and up-regulation of pro-apoptotic Bax/Bcl-2 ratio, Oncol. Rep. 17 (2) (2007) 425–431.

[13] R.J. Morrow, N. Etemadi, B. Yeo, M. Ernst, Challenging a misnomer? The role of inflammatory pathways in inflammatory breast cancer, Mediat. Inflamm. 2017 (2017) 4754827, https://doi.org/10.1155/2017/4754827.

[14] O. Habanjar, R. Bingula, C. Decombat, M. Diab-Assaf, F. Caldefie-Chezet, L. Delort, Crosstalk of inflammatory cytokines within the breast tumor microenvironment, Int. J. Mol. Sci. 24 (4) (2023), https://doi.org/10.3390/ijms24044002.

[15] N. Singh, S. Gupta, S. Rashid, A. Saraya, Association of inflammatory markers with the disease & mutation status in pancreatic cancer, The Indian journal of medical research 155 (1) (2022) 49–55, https://doi.org/10.4103/ijmr.IJMR_2238_18.

[16] D.K. Tobias, A.O. Akinkuolie, P.D. Chandler, P.R. Lawler, J.E. Manson, J.E. Buring, et al., Markers of inflammation and incident breast cancer risk in the women's health study, Am. J. Epidemiol. 187 (4) (2018) 705–716, https://doi.org/10.1093/aje/kwx250.

[17] H.A. Yıldız, M.D. Değer, G. Aslan, Prognostic value of preoperative inflammation markers in non-muscle invasive bladder cancer, Int. J. Clin. Pract. 75 (6) (2021) e14118, https://doi.org/10.1111/ijcp.14118.

[18] T. Kaur, A. Madgulkar, M. Bhalekar, K. Asgaonkar, Molecular docking in formulation and development, Curr. Drug Discov. Technol. 16 (1) (2019) 30–39, https://doi.org/10.2174/1570163815666180219112421.

[19] L. Pinzi, G. Rastelli, Molecular docking: shifting paradigms in drug discovery, Int. J. Mol. Sci. 20 (18) (2019), https://doi.org/10.3390/ijms20184331.

[20] C. Nogales, Z.M. Mamdouh, M. List, C. Kiel, A.I. Casas, H. Schmidt, Network pharmacology: curing causal mechanisms instead of treating symptoms, Trends Pharmacol. Sci. 43 (2) (2022) 136–150, https://doi.org/10.1016/j.tips.2021.11.004.

[21] L. Zhao, H. Zhang, N. Li, J. Chen, H. Xu, Y. Wang, et al., Network pharmacology, a promising approach to reveal the pharmacology mechanism of Chinese medicine formula, J. Ethnopharmacol. 309 (2023) 116306, https://doi.org/10.1016/j.jep.2023.116306.

[22] A.S. Azmi, Adopting network pharmacology for cancer drug discovery, Curr. Drug Discov. Technol. 10 (2) (2013) 95–105, https://doi.org/10.2174/1570163811310020002.

[23] X. Xu, Z. Yu, S. Zeng, Investigating the therapeutic mechanism of Xiaotan Sanjie Formula for gastric cancer via network pharmacology and molecular docking: a review, Medicine (Baltim.) 102 (46) (2023) e35986, https://doi.org/10.1097/md.0000000000035986.

[24] H. Yan, Y. Li, B. Yang, F. Long, Z. Yang, D. Tang, Exploring the mechanism of action of Yiyi Fuzi Baijiang powder in colorectal cancer based on network pharmacology and molecular docking studies, Biotechnol. Genet. Eng. Rev. (2023) 1–21, https://doi.org/10.1080/02648725.2023.2167765.

[25] M.H. Ung, F.S. Varn, C. Cheng, In silico frameworks for systematic pre-clinical screening of potential anti-leukemia therapeutics, Expert Opin Drug Discov 11 (12) (2016) 1213–1222, https://doi.org/10.1080/17460441.2016.1243524.

[26] W. Zhang, W. Tian, Y. Wang, X. Jin, H. Guo, Y. Wang, et al., Explore the mechanism and substance basis of Mahuang FuziXixin Decoction for the treatment of lung cancer based on network pharmacology and molecular docking, Comput. Biol. Med. 151 (Pt A) (2022) 106293, https://doi.org/10.1016/j.compbiomed.2022.106293.

[27] Y. Zhang, Z. Li, J. Wei, L. Kong, M. Song, Y. Zhang, et al., Network pharmacology and molecular docking reveal the mechanism of Angelica dahurica against Osteosarcoma, Medicine (Baltim.) 101 (44) (2022) e31055, https://doi.org/10.1097/md.0000000000031055.

[28] N.Z. Ismail, M. Khairuddean, S. Abubakar, H. Arsad, Network pharmacology, molecular docking and molecular dynamics simulation of chalcone scaffold-based compounds targeting breast cancer receptors, J. Biomol. Struct. Dyn. (2023) 1–16, https://doi.org/10.1080/07391102.2023.2296606.

[29] H. Zhou, Y. Zhang, C. Gan, X. Fan, Z. Qi, S. Qi, Eriocitrin suppresses proliferation and migration of hepatocellular carcinoma SMMC-7721 cells by promoting ROS production and activating the MAPK pathway, Nan Fang Yi Ke Da Xue Xue Bao 43 (3) (2023) 412–419, https://doi.org/10.12122/j.issn.1673-4254.2023.03.11.

[30] Y.C. Tsai, S.H. Chen, L.C. Lin, S.L. Fu, Anti-inflammatory principles from sarcandra glabra, J. Agric. Food Chem. 65 (31) (2017) 6497–6505, https://doi.org/10.1021/acs.jafc.6b05125.

[31] W.D. Mahauad-Fernandez, W. Naushad, T.D. Panzner, A. Bashir, G. Lal, C.M. Okeoma, BST-2 promotes survival in circulation and pulmonary metastatic seeding of breast cancer cells, Sci. Rep. 8 (1) (2018) 17608, https://doi.org/10.1038/s41598-018-35710-y.

[32] G. Xiao, X. Wang, J. Wang, L. Zu, G. Cheng, M. Hao, et al., CXCL16/CXCR6 chemokine signaling mediates breast cancer progression by pERK1/2-dependent mechanisms, Oncotarget 6 (16) (2015) 14165–14178, https://doi.org/10.18632/oncotarget.3690.

[33] P. Chen, H. Zuo, H. Xiong, M.J. Kolar, Q. Chu, A. Saghatelian, et al., Gpr132 sensing of lactate mediates tumor-macrophage interplay to promote breast cancer metastasis, Proc. Natl. Acad. Sci. U.S.A. 114 (3) (2017) 580–585, https://doi.org/10.1073/pnas.1614035114.

[34] M.H. Kaarvatn, J. Vrbanec, A. Kulic, J. Knezevic, B. Petricevic, S. Balen, et al., Single nucleotide polymorphism in the interleukin 12B gene is associated with risk for breast cancer development, Scand. J. Immunol. 76 (3) (2012) 329–335, https://doi.org/10.1111/j.1365-3083.2012.02736.x.

[35] M. Farbod, S.A. Dastgheib, F. Asadian, M. Karimi-Zarchi, S. Sayad, M. Barahman, et al., Association of IL-8 -251T>A and IL-18 -607C>A polymorphisms with susceptibility to breast cancer - a meta-analysis, Klin. Onkol. : casopis Ceske a Slovenske onkologicke spolecnosti 35 (3) (2022) 181–189, https://doi.org/10.48095/ccko2022181.

[36] R. Lappano, M. Talia, F. Cirillo, D.C. Rigiracciolo, D. Scordamaglia, R. Guzzi, et al., The IL1β-IL1R signaling is involved in the stimulatory effects triggered by hypoxia in breast cancer cells and cancer-associated fibroblasts (CAFs), J. Exp. Clin. Cancer Res. : CR 39 (1) (2020) 153, https://doi.org/10.1186/s13046-020-01667-y.

[37] L. He, W. Zhang, S. Yang, W. Meng, X. Dou, J. Liu, et al., Impact of genetic variants in IL-2RA and IL-2RB on breast cancer risk in Chinese Han women, Biochem. Genet. 59 (3) (2021) 697–713, https://doi.org/10.1007/s10528-021-10029-y.

[38] N. Meyer-Schaller, S. Tiede, R. Ivanek, M. Diepenbruck, G. Christofori, A dual role of Irf1 in maintaining epithelial identity but also enabling EMT and metastasis formation of breast cancer cells, Oncogene 39 (24) (2020) 4728–4740, https://doi.org/10.1038/s41388-020-1326-0.

[39] Q. Lan, S. Peyvandi, N. Duffey, Y.T. Huang, D. Barras, W. Held, et al., Type I interferon/IRF7 axis instigates chemotherapy-induced immunological dormancy in breast cancer, Oncogene 38 (15) (2019) 2814–2829, https://doi.org/10.1038/s41388-018-0624-2.

[40] G. Xie, H. Yang, D. Ma, Y. Sun, H. Chen, X. Hu, et al., Integration of whole-genome sequencing and functional screening identifies a prognostic signature for lung metastasis in triple-negative breast cancer, Int. J. Cancer 145 (10) (2019) 2850–2860, https://doi.org/10.1002/ijc.32329.

[41] F. Al Qutami, W. Al Halabi, M.Y. Hachim, Identification of breast cancer LCK proto-oncogene as a master regulator of TNBC neutrophil enrichment and polarization, Int. J. Mol. Sci. 24 (17) (2023), https://doi.org/10.3390/ijms241713269.

[42] D. Huang, X. Chen, X. Zeng, L. Lao, J. Li, Y. Xing, et al., Targeting regulator of G protein signaling 1 in tumor-specific T cells enhances their trafficking to breast cancer, Nat. Immunol. 22 (7) (2021) 865–879, https://doi.org/10.1038/s41590-021-00939-9.

[43] F. Xu, G. Zhou, S. Han, W. Yuan, S. Chen, Z. Fu, et al., Association of TNF-α, TNFRSF1A and TNFRSF1B gene polymorphisms with the risk of sporadic breast cancer in northeast Chinese Han women, PLoS One 9 (7) (2014) e101138, https://doi.org/10.1371/journal.pone.0101138.

[44] J.D. Merriman, B.E. Aouizerat, J.K. Cataldo, L. Dunn, B.A. Cooper, C. West, et al., Association between an interleukin 1 receptor, type I promoter polymorphism and self-reported attentional function in women with breast cancer, Cytokine 65 (2) (2014) 192–201, https://doi.org/10.1016/j.cyto.2013.11.003.

[45] N. Mavaddat, K. Michailidou, J. Dennis, M. Lush, L. Fachal, A. Lee, et al., Polygenic risk scores for prediction of breast cancer and breast cancer subtypes, Am. J. Hum. Genet. 104 (1) (2019) 21–34, https://doi.org/10.1016/j.ajhg.2018.11.002.

[46] M. Kiely, B. Lord, S. Ambs, Immune response and inflammation in cancer health disparities, Trends in cancer 8 (4) (2022) 316–327, https://doi.org/10.1016/j.trecan.2021.11.010.

[47] B. Lin, L. Du, H. Li, X. Zhu, L. Cui, X. Li, Tumor-infiltrating lymphocytes: warriors fight against tumors powerfully, Biomedicine & pharmacotherapy = Biomedecine & pharmacotherapie 132 (2020) 110873, https://doi.org/10.1016/j.biopha.2020.110873.

[48] J.A. Espinoza, S. Jabeen, R. Batra, E. Papaleo, V. Haakensen, Wielenga V. Timmermans, et al., Cytokine profiling of tumor interstitial fluid of the breast and its relationship with lymphocyte infiltration and clinicopathological characteristics, OncoImmunology 5 (12) (2016) e1248015, https://doi.org/10.1080/2162402x.2016.1248015.

[49] H. Qayoom, S. Sofi, M.A. Mir, Targeting tumor microenvironment using tumor-infiltrating lymphocytes as therapeutics against tumorigenesis, Immunol. Res. 71 (4) (2023) 588–599, https://doi.org/10.1007/s12026-023-09376-2.

[50] G. Gao, Z. Wang, X. Qu, Z. Zhang, Prognostic value of tumor-infiltrating lymphocytes in patients with triple-negative breast cancer: a systematic review and meta-analysis, BMC Cancer 20 (1) (2020) 179, https://doi.org/10.1186/s12885-020-6668-z.

[51] C. Denkert, G. von Minckwitz, S. Darb-Esfahani, B. Lederer, B.I. Heppner, K.E. Weber, et al., Tumour-infiltrating lymphocytes and prognosis in different subtypes of breast cancer: a pooled analysis of 3771 patients treated with neoadjuvant therapy, Lancet Oncol. 19 (1) (2018) 40–50, https://doi.org/10.1016/s1470-2045 (17)30904-x.

[52] P. Savas, R. Salgado, C. Denkert, C. Sotiriou, P.K. Darcy, M.J. Smyth, et al., Clinical relevance of host immunity in breast cancer: from TILs to the clinic, Nat. Rev. Clin. Oncol. 13 (4) (2016) 228–241, https://doi.org/10.1038/nrclinonc.2015.215.

[53] H. Zhou, Y.D. Tang, C. Zheng, Revisiting IRF1-mediated antiviral innate immunity, Cytokine Growth Factor Rev. 64 (2022) 1–6, https://doi.org/10.1016/j. cytogfr.2022.01.004.

[54] L. Shao, W. Hou, N.E. Scharping, F.P. Vendetti, R. Srivastava, C.N. Roy, et al., IRF1 inhibits antitumor immunity through the upregulation of PD-L1 in the tumor cell, Cancer Immunol. Res. 7 (8) (2019) 1258–1266, https://doi.org/10.1158/2326-6066.Cir-18-0711.

[55] H. Sato, A. Niimi, T. Yasuhara, T.B.M. Permata, Y. Hagiwara, M. Isono, et al., DNA double-strand break repair pathway regulates PD-L1 expression in cancer cells, Nat. Commun. 8 (1) (2017) 1751, https://doi.org/10.1038/s41467-017-01883-9.

[56] K. Gao, Q. Shi, Y. Gu, W. Yang, Y. He, Z. Lv, et al., SPOP mutations promote tumor immune escape in endometrial cancer via the IRF1-PD-L1 axis, Cell Death Differ. 30 (2) (2023) 475–487, https://doi.org/10.1038/s41418-022-01097-7.

Abbreviation

BRCA: Breast cancer
TCM: Traditional Chinese Medicine;
TCMID: Traditional Chinese Medicine integrative database
TCMSP: Traditional Chinese Medicine Systems Pharmacology
GO: Gene ontology
DO: Disease ontology
KEGG: Kyoto encyclopedia of genes
CCK-8: Cell counting kit-8
IHC: Immunohistochemical
IF: Immunofluorescence
DEGs: Differentially expressed genes
TCGA: The cancer genome atlas
GEO: Gene Expression Omnibus
Co-IP: Co-immunoprecipitation
SD: Standard deviation
PD-L1: Programmed death-ligand 1
STAT3: Signal transducer and activator of transcription 3
IRF1: Interferon regulatory factor 1